Supporting Information

Designed construction of yolk-shell structured trimanganese tetraoxide nanospheres via polar solvent-assisted etching and biomass-derived activated porous carbon materials for high-performance asymmetric supercapacitors

Goli Nagaraju,[a] *S. Chandra Sekhar,*[a] *G. Seeta Rama Raju,*[b] *L. Krishna Bharat,*[a] *and Jae Su Yu*[a*]

[a]Department of Electronics and Radio Engineering, Institute for Wearable Convergence Electronics, Kyung Hee University, 1 Seocheon-dong, Giheung-gu, Yongin-si, Gyeonggi-do 446-701, Republic of Korea.

[b]Department of Energy and Materials Engineering, Dongguk University-Seoul, Seoul 04620, Republic of Korea.

*Address correspondence to jsyu@khu.ac.kr

Tel: +82-31-201-3820; Fax: +82-31-206-2820

Table S1. Crystallographic and atomic parameters of the yolk-shell structured Mn_3O_4 NSs from Rietveld refinement.

Atom	**Site**	**x**	**y**	**z**	**Occ**
O	16h	0.0	0.52507	0.23844	0.48247
Mn^{2+}	4a	0.0	0.0	0.0	0.24901
Mn^{3+}	8d	0.0	0.25	0.375	0.12538
Lattice Parameters			**R-Factors**		
a (Å)	5.7635		R_{wp}	2.69	
b (Å)	5.7635		R_p	3.39	
c (Å)	9.4503		R_{exp}	4.09	
V ($Å^3$)	313.9195		χ^2	0.686	

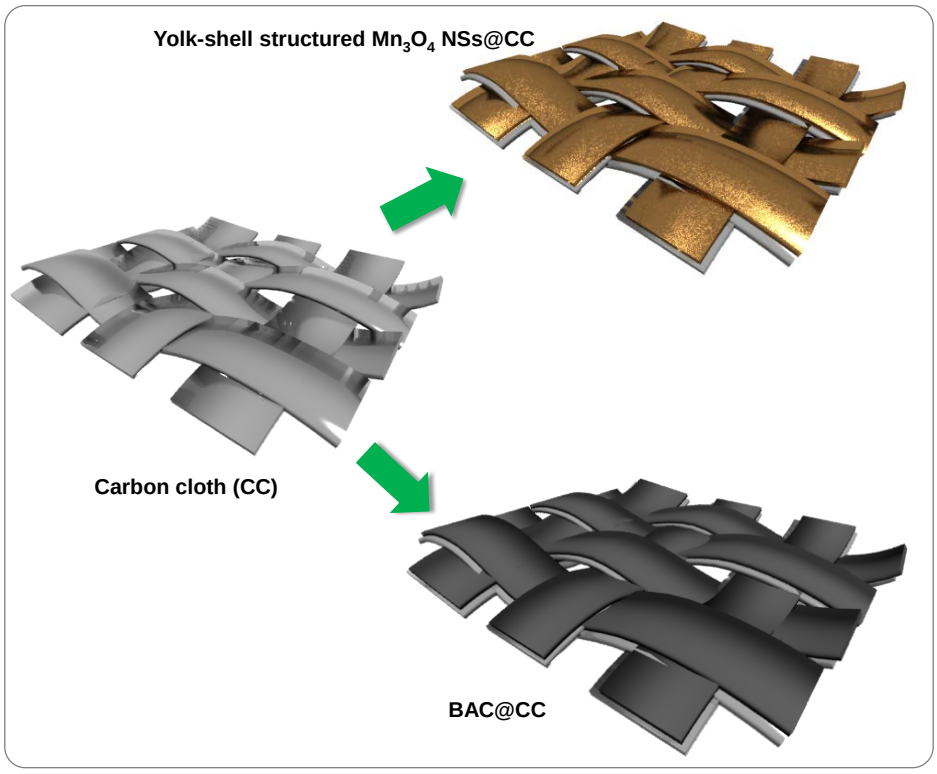

Figure S1. Schematic diagram for the coating process of both positive and negative electrode materials for electrochemical tests.

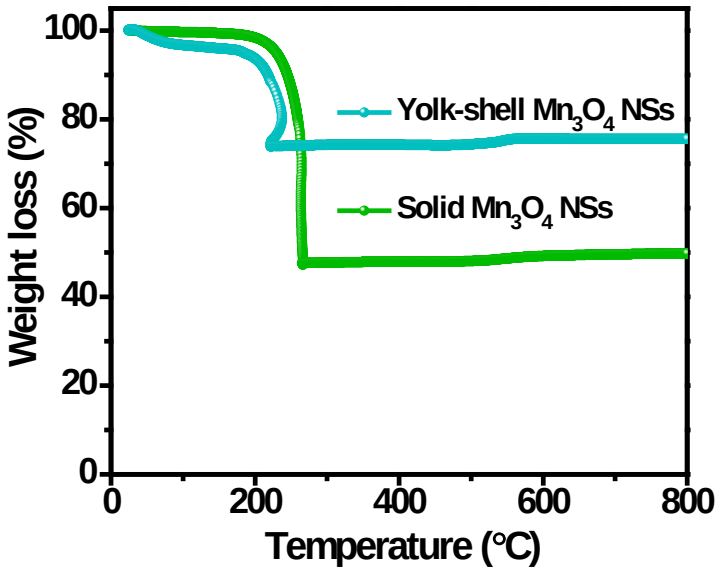

Figure S2. TGA analysis of the solid and yolk-shell structured Mn_3O_4 NSs.

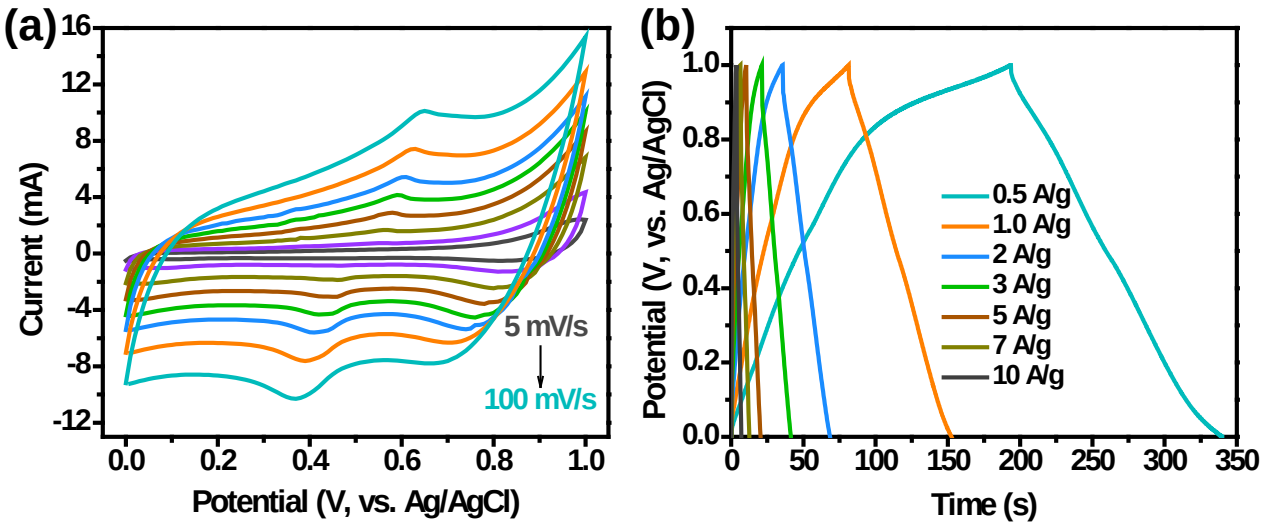

Figure S3. (a) CV curves and (GCD) curves of solid Mn_3O_4 NSs electrode measured at different scan rates and current densities in 1 M Na_2SO_4 electrolyte using the three-electrode system.

The surface analysis of the BAC powder was carried out using BET N_2 adsorption/desorption isotherms. As shown in Figure S4, N_2 adsorption/desorption isotherm of BAC displays a typical type-IV isotherm (based on the IUPAC classification) with a mesoporous property. Specifically, a sharp rise at low relative pressure (P/P_0) demonstrates that the BAC made up of large quantities of micropores. Also, the following slope values at 0.43 to 1.0 further shows the macroporous and well-developed mesoporous structures in the BAC powder. The obtained surface area of BAC was 1950.9 m^2g^{-1}, respective as calculated by the BET method. Meanwhile, the pore size distribution spectrum is shown in the inset of Figure S4, confirming the presence of hierarchical porosity with rich micropores and limited mesopores. The average pore diameter and total pore volume of BAC were about 2.88 nm and 1.41 cm^3 g^{-1}, respectively. Such high surface area and porous nature of BAC could be expected to provide rapid electrolyte ion diffusion paths and surface reactions during electrochemical measurements.

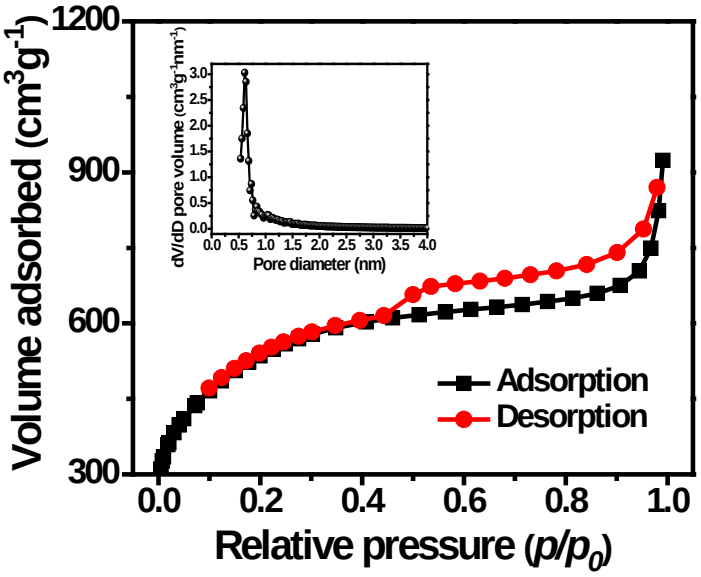

Figure S4. N_2 adsorption/desorption isotherm and pore size distribution curves of the waste box derived activated porous carbon.

Table S2. Comparitive electrochemical performances of the yolk-shell structured Mn_3O_4 NSs with previously reported manganese-based nanomaterials using the three-electrode system in aqueous electrolyte solution.

Electrode material	Current collector	Synthesis method	Electrolyte solution	Test condition	Mass loading	C_{sp}	Ref.
Mn_3O_4@rGO composites	Stainless steel mesh	Microwave hydrothermal method	1 M Na_2SO_4	5 mV s^{-1}	3 mg/cm^2	153 F g^{-1}	[S1]
Graphene@Mn_3O_4 composites	Stainless steel foil	Solvothermal synthesis	1 M Na_2SO_4	0.1 A g^{-1}	--	147 F g^{-1}	[S2]
$MnCO_3$ nanospheres and nanocubes	Ni foam	Co-precipitation method	0.1 M $NaClO_4$	0.15 A g^{-1}	--	129 and 90 F g^{-1}	[S3]
Mn_3O_4 nanoparticles embedded graphene	Pt foil	Organosol-Ultrasonciation	1 M Na_2SO_4	5 mV s^{-1}	0.75 mg/cm^2	175 F g^{-1}	[S4]
Cube-like Mn_3O_4@rGO	Stainless steel mesh	Chemical decomposition	1 M Na_2SO_4	0.5 A g^{-1}	--	131 F g^{-1}	[S5]
Mn_3O_4 nanorods@ graphene	Ni foam	Solvothermal	1 M Na_2SO_4	1 A g^{-1}	2 mg/cm^2	115 F g^{-1}	[S6]
Mn_3O_4 nanowires	Graphite paper	Hydrothermal method	1 M Na_2SO_4	500 mV s^{-1}	0.25 mg/cm^2	170 F g^{-1}	[S7]
Porous MnO/Mn_3O_4 composites	Carbon disk	Mn oleate decomposition	1 M Na_2SO_4	1 A g^{-1}	0.15 mg/cm^2	207 F g^{-1}	[S8]
Mn_3O_4@rGO composites	Graphite substrate	Microwave-assisted hydrothermal	0.5 M Na_2SO_4	25 mV s^{-1}	0.5 mg/cm^2	193 F g^{-1}	[S9]
Hollow Mn_3O_4 structures	Glassy carbon	Hydrothermal method	2 M KCl	5 mV s^{-1}	--	148 F g^{-1}	[S10]
Mn_3O_4 nanosheets	Carbon fiber paper	Electrodeposition	2 M KCl	10 mV s^{-1}	1.1 mg/cm^2	145 F g^{-1}	[S11]
Porous Mn_3O_4 nanoplates	Ni foam	Hydrothermal method	1 M Na_2SO_4	0.5 A g^{-1}	--	82 F g^{-1}	[S12]
Yolk-shell structured Mn_3O_4 NSs	Carbon cloth	Solvothermal hydrolysis	1 M Na_2SO_4	0.5 A g^{-1}	1.6 mg/cm^2	211.36 F g^{-1}	This work

References

S1. L. Li, K. H. Seng, H. Liu, I. P. Nevirkovets and Z. Guo, Electrochim. Acta, 2013, 87, 801-808.

S2. X. Zhang, X. Sun, Y. Chen, D. Zhang and Y. Ma, Mater. Lett., 2012, 68, 336-339.

S3. N. Zhang, J. Ma, Q. Li, J. Li and D. H. L. Ng, RSC Adv., 2015, 5, 81981-81985.

S4. B. Wang, J. Park, C. Wang, H. Ahn and G. Wang, Electrochim. Acta, 2010, 55, 6812-6817.

S5. K. Subramani, D. Jeyakumar and M. Sathish, Phys. Chem. Chem. Phys., 2014, 16, 4952-4961.

S6. J. W. Lee, A. S. Hall, J.-D. Kim and T. E. Mallouk, Chem. Mater., 2012, 24, 1158-1164.

S7. C.-C. Hu, Y.-T. Wu and K.-H. Chang, Chem. Mater., 2008, 20, 2890-2894.

S8. J. Yang, X. Yang, Y. L. Zhong and J. Y. Ying, Nano Energy, 2015, 13, 702-708.

S9. C.-L. Liu, K.-H. Chang, C.-C. Hu and W.-C. Wen, J. Power Sources, 2012, 217, 184-192.

S10. M. Fang, X. Tan, M. Liu, S. Kang, X. Hu and L. Zhang, CrystEngComm, 2011, 13, 4915-4920.

S11. K.-W. Nam, M. G. Kim and K.-B. Kim, J. Phys. Chem. C, 2007, 111, 749-758.

S12. Z. Liu, Y. Xing, S. Fang, X. Qu, D. Wu, A. Zhang and B. Xu, RSC Adv., 2015, 5, 54867-54872.